J Appl Electrochem (2007) 37:819–826
DOI 10.1007/s10800-007-9317-1

ORIGINAL PAPER

The effect of poly(vinyl caprolactone-co-vinyl pyridine) and poly(vinyl imidazol-co-vinyl pyridine) on the corrosion of steel in H_3PO_4 media

M. Benabdellah · A. Ousslim · B. Hammouti · A. Elidrissi · A. Aouniti · A. Dafali · K. Bekkouch · M. Benkaddour

Received: 23 March 2006 / Accepted: 20 February 2007 / Published online: 24 March 2007

Abstract The inhibiting effect of two organic copolymers namely poly(vinyl caprolactone-co-vinyl pyridine) (PVCVP) and poly(vinyl imidazol-co-vinyl pyridine) (PVIVP) on the corrosion of steel in phosphoric acid was investigated at various temperatures. The study was carried out by potentiodynamic polarization, electrochemical impedance spectroscopy (EIS) and weight loss measurements. Inhibition efficiency (E %) increased with polymer concentration to attain 85% at 10^{-4} M for PVIVP. Adsorption of polymers on the steel surface in 2 M H_3PO_4 followed the Langmuir isotherm model. EIS measurements show that the dissolution of steel occurs under activation control. Polarisation curves indicate that the tested polymers functioned as cathodic inhibitors. E % values obtained from various methods used are in good agreement with each other. The temperature effect on the corrosion behaviour of steel in 2 M H_3PO_4 in the presence and absence of the inhibitor was studied in the temperature range 298–338 K. The adsorption free energy (ΔG^{o}_{ads}) and the activation parameters (E_a, ΔH^{o}_{a}, ΔS^{o}_{a}) for the steel dissolution reaction in the presence of polymer were determined.

Keywords Polymer · Steel · Phosphoric acid · Corrosion inhibition · Adsorption

M. Benabdellah · A. Ousslim · B. Hammouti (✉) · A. Elidrissi · A. Aouniti · A. Dafali · K. Bekkouch · M. Benkaddour
Laboratoire de Chimie Appliquée et Environnement, Faculté des Sciences, B.P. 717 Oujda, Morocco
e-mail: hammoutib@yahoo.fr

1 Introduction

The adsorption modes of organic inhibitors depend mainly on the chemical structure of the inhibitor, the chemical composition of the solution, the nature of the metal surface and the electrochemical potential of the metal-solution interface. Numerous works have been devoted to the corrosion inhibiting effect of aqueous soluble polymers on metallic materials. Polyvinyl pyridine and their derivatives, polyvinylimidazoles, polyethylenimine, polyaniline, polypyrrole and polyurethane have been widely examined [1–12]. The inhibitive action of polymers is structurally related in most cases to the various active centres of adsorption such as cyclic rings and heteroatoms such as oxygen and nitrogen.

Most organic inhibitors act by adsorption on the metal surface [13], N-heterocyclic compounds such as imidazole [14–20] and pyridine derivatives [21–25] inhibit the corrosion of many metals in acidic solutions with good protection. A thermodynamic model is an important tool for studying the mechanism of inhibition. In this context a thermodynamic model for the adsorption process has been suggested [26, 27].

The objective of this work is to study the inhibiting effect of two polymers on the corrosion inhibition of steel in phosphoric acid solution at various temperatures using polarisation, EIS and gravimetric measurements. The kinetic and adsorption parameters have been evaluated.

2 Experimental

2.1 Inhibitors

The monomers: 1-vinyl-imidazole, 4-vinyl-caprolactone and 4-vinyl-pyridine were obtained from Aldrich and were

used as received. Azo-bis isobutyronitril (AIBN) was crystallized from chloroform before use; the solvents were of analytical or spectroscopic grade.

Copolymerisation was achieved according to the procedure reported elsewhere [28–30]: the copolymerisation of vinyl-imidazole and vinyl-caprolactone with 4-vinyl pyridine were carried out in bulk under argon atmosphere, equal quantities of the two monomers and some AIBN (0.8 wt% with respect to monomer) were placed in a standard reaction tube and the mixture was purged with argon gas for deoxygenation. The mixture was stirred for 3 h in a thermostat maintained at 333 K, exposed to UV light and subsequently poured in *n*-hexane. The precipitated copolymers were filtered, washed and dried under vacuum at 333 K for 24 h. The units of each monomer are randomly distributed along the copolymer chain (Fig. 1). The structures of the copolymers (1) and (2) were confirmed by IR and NMR analysis and their molecular weights determined by the viscosity technique.

2.2 Electrochemical and gravimetric measurements

A solution of 2 M H_3PO_4 was prepared by dilution of analytical grade 85% H_3PO_4 with double-distilled water. Prior to all measurements, the steel samples (0.09% P, 0.38% Si, 0.01% Al, 0.05% Mn, 0.21% C, 0.05% S and the remainder iron) were polished with emery paper up to 1,200 grade, washed thoroughly with double-distilled water, degreased with AR grade ethanol, acetone and dried at room temperature.

Electrochemical measurements were carried out in a conventional three-electrode electrolysis cylindrical Pyrex glass cell. The working electrode (WE), in the form of disc had a geometric area of 1 cm^2 and was embedded in poly tetrafluoroethylene (PTFE). A saturated calomel electrode (SCE) and a platinum disc electrode were used respectively, as reference and auxiliary electrodes. The temperature was thermostatically controlled at 298 ± 1 K. The WE was abraded with silicon carbide paper (grade P1200), degreased with acetone and rinsed with double-distilled water before use.

Electrochemical polarization tests were conducted using EG & G Instruments potentiostat–galvanostat model 263A at a scan rate of 0.5 mV s^{-1} and the data analysed using the 352 Soft Corr^{TM} III Software. Before recording the cathodic polarisation curves, the steel electrode was polarised at –800 mV for 10 min. The potential of the electrode was swept from –800 mV to more positive values. The test solution was deaerated throughout the experiments by bubbling with pure nitrogen.

Electrochemical impedance spectroscopy (EIS) was undertaken with an electrochemical system (Tacussel) which included a digital potentiostat model Voltalab PGZ 100. Measurements were carried out at E_{corr} after 30 min of exposure to the test solution. Sine wave voltages (10 mV) peak to peak, at frequencies between 100 kHz and 10 mHz were superimposed on the rest potential. The impedance diagrams are given as Nyquist plots. Values of R_t and C_{dl} were obtained.

Gravimetric measurements were carried out in a double walled glass cell equipped with a thermostat-cooling condenser. The solution volume was 60 ml and the pre-weighed steel samples used were in rectangular form, with dimensions (2.5 × 2 × 0.05 cm). The immersion time for the weight loss was 2 h at 298 K and 1 h at other temperatures. After the corrosion test, the specimens were carefully washed in double-distilled water, dried and then weighed. Triplicate experiments were performed in each case and the mean value of the weight loss is reported. The mean corrosion rate as expressed in mg cm^{-2} h^{-1}.

3 Results and discussion

3.1 Polarisation measurements

The polarisation curves of steel in 2 M H_3PO_4 in the absence and presence of PVCVP and PVIVP at different concentrations at 298 K are presented in Figs. 2 and 3. The collected parameters deduced from the polarisation curves such as the corrosion potential (E_{corr}), corrosion current (I_{corr}), cathodic Tafel slopes (β_c) and percentage inhibition

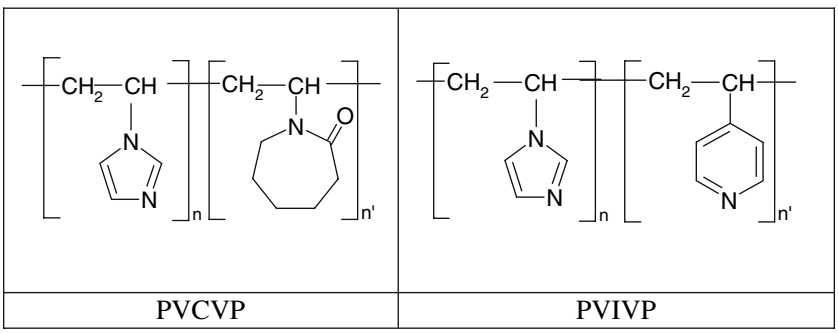

Fig. 1 Chemical formula of copoly(vinyl caprolactone-vinyl pyridine) (Poly1 PVCVP) and Copoly(vinyl imidazol -vinyl pyridine) (Poly2 PVIVP)

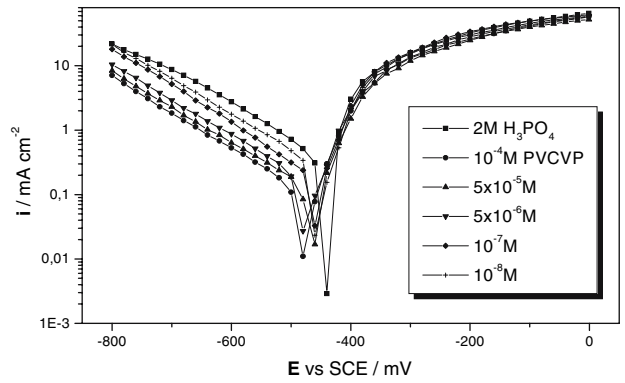

Fig. 2 Polarisation curves of steel in 2 M H_3PO_4 at various concentrations of PVCVP

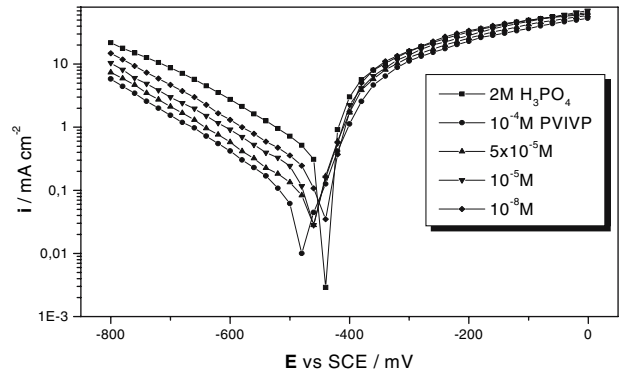

Fig. 3 Polarisation curves of steel in 2 M H_3PO_4 at various concentrations of PVIVP

efficiency (E_I %) are shown in Table 1. Equation (1) determines the inhibition efficiency (E_I %):

$$E_I\% = \frac{I_{corr} - I_{corr(inh)}}{I_{corr}} \times 100 \quad (1)$$

where I_{corr} and $I_{corr\ (inh)}$ are corrosion current densities without and with the inhibitor, respectively, determined by extrapolation of the cathodic Tafel lines to the corrosion potential.

The cathodic current-potential curves give rise to Tafel lines indicating that the hydrogen evolution reaction is activation controlled. The cathodic current density decreases with the concentration of PVCVP and PVIVP. The slopes of the cathodic Tafel lines b_c and the corrosion potential remain almost constant with increase in inhibitor concentration. This suggests that the mechanism of reduction of hydrogen ions is not modified in the presence of PVCVP and PVIVP. In the anodic domain however, the i-E characteristics are almost the same. This indicates that the polymers act predominantly as cathodic inhibitors by simple blocking the available surface area. The inhibitor molecules decrease the surface area of corrosion and only cause inactivation of part of the surface with respect to the corrosion medium [31].

3.2 Electrochemical impedance spectroscopy (EIS)

EIS was carried out on a newly polished steel surface in acidic solution in the absence and presence of inhibitor at open circuit potential at 298 K after 30 min of immersion. Nyquist plots of steel in uninhibited and inhibited acid solutions containing various concentrations of polymers are shown in Figs. 4 and 5. The impedance diagrams obtained are not perfect semicircles and this difference has been attributed to the frequency dispersion [32].

The charge transfer resistance, (R_t) values were calculated from the difference in impedance at lower and higher frequencies. To obtain the double capacitance (C_{dl}), the frequency at which the imaginary component of the

Table 1 Electrochemical parameters of steel at various concentrations of polymers 1 and 2 in 2 M H_3PO_4 and corresponding inhibition efficiency

	Concentration (M)	E_{corr} versus SCE (mV)	b_c (mV dec^{-1})	I_{corr} (μA cm^{-2})	E (%)
Blank	2	–465	198.4	533.0	–
PVCVP	10^{-4}	–485	177.3	119.0	78
	5×10^{-5}	–479	183.1	148.0	72
	10^{-5}	–480	187.7	182.3	66
	5×10^{-6}	–484	199.5	199.5	63
	10^{-7}	–478	170.4	246.1	54
	10^{-8}	–475	184.1	372.5	30
PVIVP	10^{-4}	–492	189.3	84.2	84
	5×10^{-5}	–483	191.6	108.2	80
	10^{-5}	–486	190.4	147.3	72
	5×10^{-6}	–480	184.2	163.1	69
	10^{-7}	–470	188.7	227.5	57
	10^{-8}	–471	186.4	253.5	52

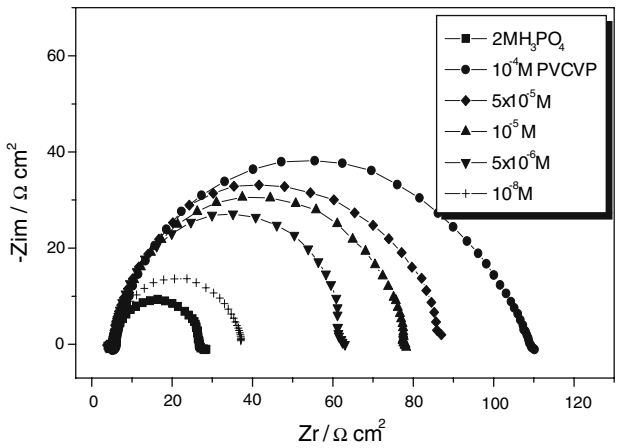

Fig. 4 Nyquist diagrams for steel in 2 M H_3PO_4 at different concentrations of PVCVP

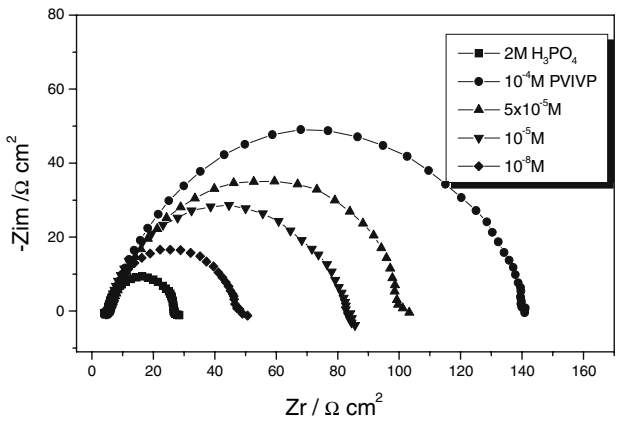

Fig. 5 Nyquist diagrams for steel in 2 M H_3PO_4 at different concentrations of PVIVP

impedance is maximum ($-Z_{max}$) was found and C_{dl} values were obtained from the equation:

$$f(-Z_{max}) = \frac{1}{2\pi C_{dl} R_t}. \quad (2)$$

The percentage inhibition efficiency was calculated from the charge-transfer resistance by the following relation:

$$E_{Rt}\% = \frac{R_t^{-1} - {}^{-1}_{t(inh)}}{R_t^{-1}} \times 100. \quad (3)$$

R_t and $R_{t\ (inh)}$ are charge transfer resistance values with and without inhibitor, respectively.

The impedance parameters derived from these investigations are given in Table 2. R_t increases with increase in polymer concentration indicating insulating adsorption layer formation. According to the Helmholtz model the double layer capacitance C_{dl} is given by:

$$C_{dl} = \frac{\varepsilon_0 \varepsilon}{\delta} S \quad (4)$$

where δ is thickness of the deposit, S surface area of the electrode, ε_o permittivity of air and ε medium dielectric constant. The decrease in C_{dl} values (Fig. 6) may be attributed either to a decrease in local dielectric constant ε [33] or to the thickness of the adsorbed inhibitor layer on the metal surface [34].

3.3 Weight loss tests

Gravimetric experiments were carried out on steel in 2 M H_3PO_4 in the absence and presence of various concentrations of PVCVP and PVIVP at 2 h of immersion and at 298 K. The inhibition efficiency (E_w %) was estimated by:

$$E_w\% = \frac{W_{corr} - W_{corr(inh)}}{W_{corr}} \times 100 \quad (5)$$

Table 2 Characteristic parameters evaluated from the impedance diagram for steel in 2 M H_3PO_4 at various concentrations of polymers 1 and 2

	Concentration (M)	R_t (Ω cm^2)	f_{max} (Hz)	C_{dl} (μF cm^{-2})	E (%)
Blank	2	20.8	89.28	85.7	–
PVCVP	10^{-4}	104.1	31.64	48.32	80
	5×10^{-5}	81.4	40	48.88	74
	10^{-5}	71.9	44.64	49.58	71
	5×10^{-6}	56.2	44.64	63.43	63
	10^{-7}	43.4	50	73.34	52
	10^{-8}	32.2	56.18	87.79	35
PVIVP	10^{-4}	133.7	25	47.61	84
	5×10^{-5}	93.1	31.64	54.02	78
	10^{-5}	76.3	40	52.14	73
	5×10^{-6}	65	35.71	68.56	68
	10^{-7}	49	50	64.96	58
	10^{-8}	42.7	50	74.54	51

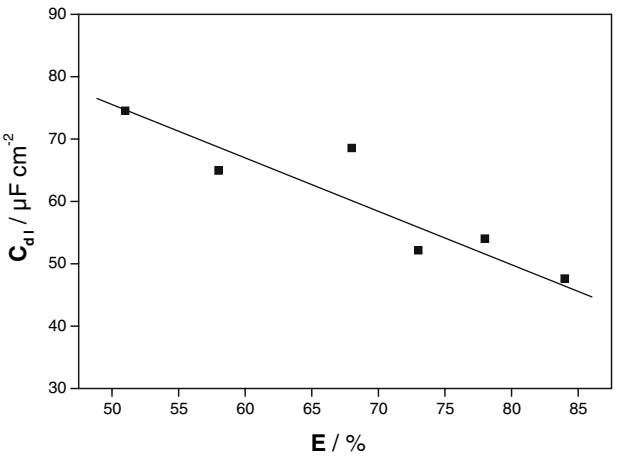

Fig. 6 Evolution of C_{dl} with the inhibition efficiency of PVIVP

where W_{corr} and $W_{corr\ (inh)}$ are the corrosion rates of steel in the absence and presence of the organic compound, respectively. Table 3 summarizes the corrosion rates and the inhibition efficiency evaluated from weight loss measurements for different inhibitor concentrations. The corrosion rate decreased with polymer concentration and in turn the inhibition efficiency (E_w %) increased to reach 85% for 10^{-4} M PVIVP. Figures 7 and 8 show the variation of corrosion rate and inhibition efficiency with polymer concentration.

3.4 Effect of temperature

The effect of temperature on the anti-corrosion effectiveness of the inhibitors studied at various concentrations in the temperature domain (308–348 K) after 1 h immersion is summarized in Table 4. The corrosion rate increased with rise in temperature for all polymer concentrations. PVIVP is also seen to be more effective than PVCVP. This may be explained by the presence of both imidazole and pyridine rings in the PVIVP molecule. Imidazole and pyridine derivatives are widely known for their inhibiting effect. The inhibition efficiency decreases with increase in temperature indicating that at higher temperature the dissolution of steel predominates over polymer adsorption.

3.5 Apparent activation energy (E_a) and pre-exponential factor (A)

It has been pointed out by Putilova et al. [35] that the logarithm of corrosion rate (W) is a linear function of 1/T as stated in the Arrhenius equation:

$$W = A \exp\left(-\frac{E_a}{RT}\right) \tag{6}$$

where E_a is apparent effective activation energy, T absolute temperature, R universal gas constant and A Arrhenius pre-exponential factor. An alternative formulation of the Arrhenius equation is the transition state equation:

$$W = \frac{RT}{Nh} \exp\left(\frac{\Delta S_a^o}{R}\right) \exp\left(-\frac{\Delta H_a^o}{RT}\right) \tag{7}$$

where h is Plank's constant, N Avogrado number and $\Delta S^o{}_a$ and ΔH_a^o are, respectively, the entropy and enthalpy of activation. Figure 9 shows the plots of ln (W) against 1/T to be straight lines with slope ($-E_a/R$). Figure 10 also presents linear plots of ln (W/T) against 1/T with a slope of $(-\Delta H_a^o/R)$ and an intercept of ($\ln R/Nh + \Delta S^o{}_a/R$), from which the values of ΔH_a^o and $\Delta S^o{}_a$ given in Table 5 were calculated.

Table 3 Gravimetric results of steel in acid without and with addition of polymers 1 and 2 at 2 h at 298 K

Inhibitors	Concentration (M)	W (mg cm^{-2} h^{-1})	E_w (%)	θ
Blank	2	1.410	–	–
PVCVP	10^{-4}	0.288	80	0.80
	5×10^{-5}	0.352	75	0.75
	10^{-5}	0.437	69	0.69
	5×10^{-6}	0.536	62	0.62
	10^{-6}	0.564	60	0.60
	10^{-7}	0.606	57	0.57
	10^{-8}	0.961	32	0.32
PVIVP	10^{-4}	0.216	85	0.85
	5×10^{-5}	0.251	82	0.82
	10^{-5}	0.356	75	0.75
	5×10^{-6}	0.405	71	0.71
	10^{-6}	0.488	65	0.65
	10^{-7}	0.558	60	0.60
	10^{-8}	0.646	54	0.54

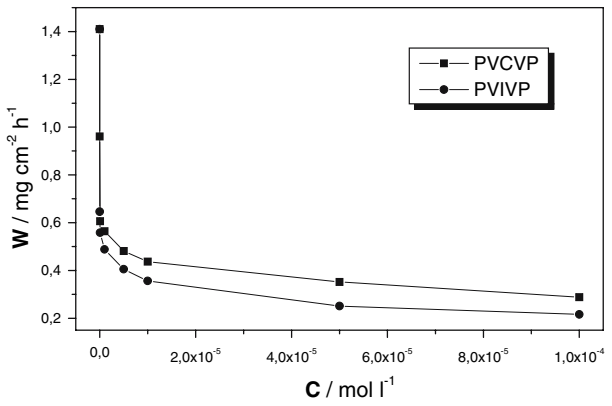

Fig. 7 Effect of concentration of polymers 1 and 2 on the corrosion rate in 2 M H_3PO_4 at 298 K

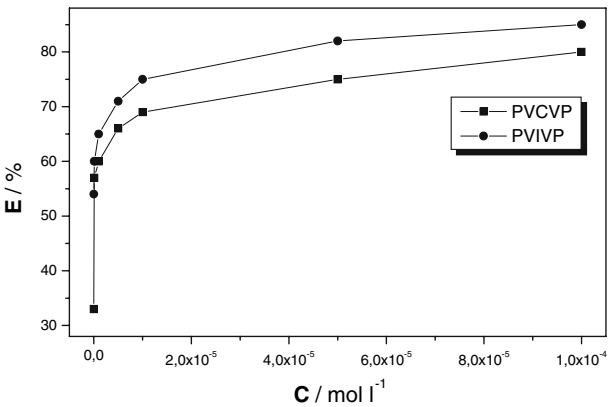

Fig. 8 Variation of inhibition efficiency with inhibitor concentration for steel in 2 M H_3PO_4 at 298 K

Table 5 also presents the calculated values of. E_a in inhibited and uninhibited acid. It is observed that the activation energy is higher in the presence of inhibitor than in its absence. An increase in E_a in the presence of the inhibitor compared to the blank, as well as a decrease in inhibition efficiency with rise in temperature, is often regarded as indicative of physical adsorption [36]. The possibility of the occurrence of both chemisorption and physical adsorption of inhibitor has also been suggested by some authors [36, 37]. This suggestion will be discussed after the determination of the adsorption parameters.

From Eq. (6), it can be seen that at a given temperature, the value of the corrosion rate is jointly decided by the activation energy and the pre-exponential factor. The decrease in corrosion rate is mostly decided by the activation energy. As clearly seen in Table 5, both E_a and A increased in the presence of inhibitor [38]. The positive sign of the enthalpy (ΔH_a^o) reflects the endothermic nature of the steel dissolution process. E_a and (ΔH_a^o) values vary in the same way with inhibitor concentration. This verifies the known thermodynamic relation between E_a and (ΔH_a^o) [39]:

$$E_a - \Delta H_a^0 = RT. \tag{8}$$

The calculate values 2.67 kJ mol^{-1} are too close to RT which is 2.48 kJ mol^{-1} at 298 K.

The entropy of activation ΔS^o_a in the absence and presence of polymers is negative. The higher values obtained in the presence of inhibitors implies that an increase in disordering takes place on going from reactants to the activated complex [40].

3.6 Adsorption isotherm and thermodynamic parameters

The dependence of the fraction of the surface covered θ on the concentration (C) of the inhibitor was tested graphically by fitting it to various isotherms. Langmuir's isotherm assumes that the solid surface contains a fixed number of adsorption sites and each site holds one adsorbed species. Figures 11 and 12 show linear plots for C/θ versus C, suggesting that adsorption obeys the Langmuir isotherm:

$$\frac{C}{\theta} = \frac{1}{K} + C \tag{9}$$

where C is inhibitor concentration, K adsorptive equilibrium constant and θ surface coverage. The standard adsorption free energy (ΔG_{ads}) was calculated using the equation [27]:

$$K = \frac{1}{55.5}\exp\left(-\frac{\Delta G^o_{ads}}{RT}\right). \tag{10}$$

Table 4 Inhibition efficiency obtained from the corrosion rate 10^{-4} M of polymers 1 and 2 in 2 M H_3PO_4 at different temperatures at 1 h

	Blank	PVCVP		PVIVP	
T (K)	W_0 (mg cm^{-2} h^{-1})	W (mg cm^{-2} h^{-1})	E (%)	W (mg cm^{-2} h^{-1})	E (%)
308	2.6	0.725	72	0.519	80
318	5.514	2.106	62	1.531	72
328	9.83	4.563	54	3.354	66
338	17.87	9.715	46	7.629	57
348	25.11	15.56	38	13.364	47

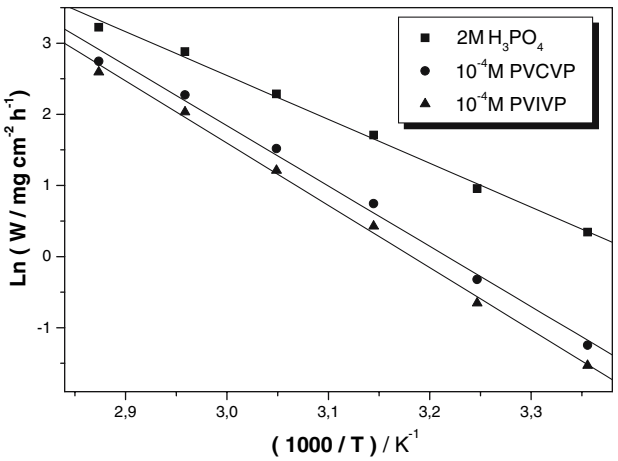

Fig. 9 Arrhenius plots of steel for 10^{-4} M of polymers in 2 M H_3PO_4

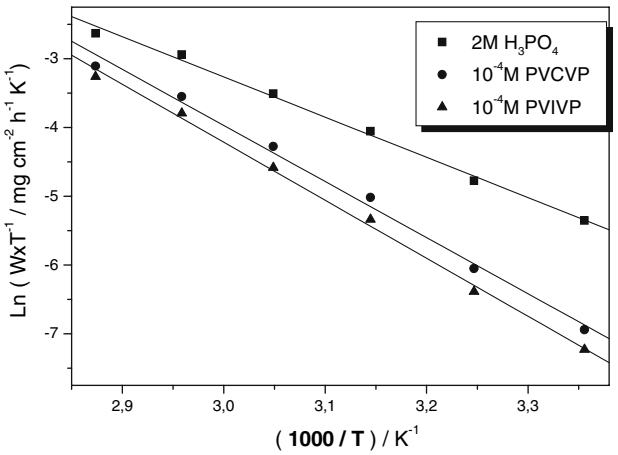

Fig. 10 Plots of log (*W*/*T*) against of T^{-1} for 10^{-4} M of polymers in 2 M H_3PO_4

The adsorption parameters are listed in Table 6. The negative values of ΔG^{o}_{ads} indicate the spontaneous adsorption on the steel surface. More negative values of ΔG^{o}_{ads} also suggest strong interaction of inhibitor molecules with the surface [41]. Generally, values of ΔG^{o}_{ads} around –20 kJ mol^{-1} or lower are consistent with the electrostatic interaction between the charged molecules and the charged metal (physisorption) while those around –40 kJ mol^{-1} or higher involve charge sharing or transfer from organic molecules to the metal surface to form a coordinate type of bond (chemisorption) [42, 43]. The calculated ΔG^{o}_{ads} values, which are more negative

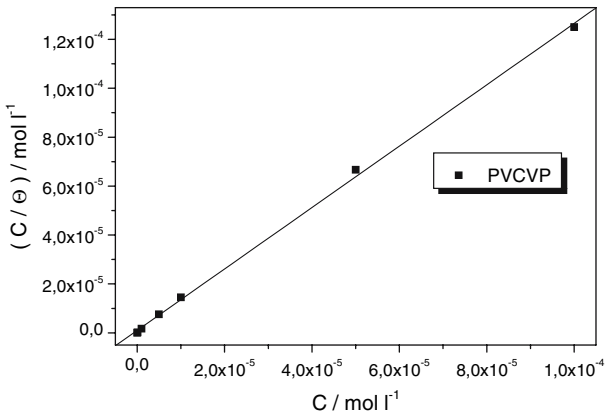

Fig. 11 Langmuir adsorption isotherm of PVCVP on steel in 2 M H_3PO_4 at 298 K

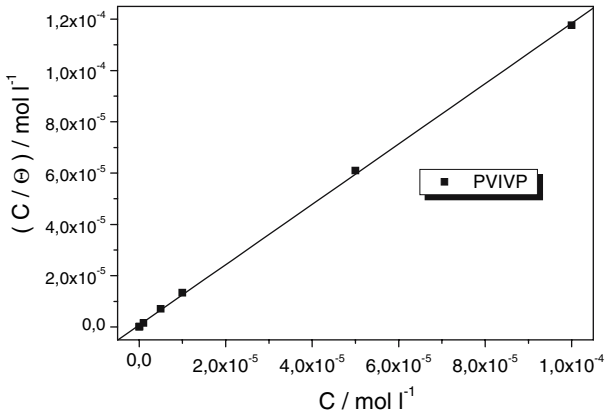

Fig. 12 Langmuir adsorption isotherm of PVIVP on steel in 2 M H_3PO_4 at 298 K

than –40 kJ mol^{-1} indicate, therefore, that the adsorption mechanism of the polymer compounds on steel in 2 M H_3PO_4 is typical of chemisorption (Table 6). The thermodynamic and activation parameters, respectively, point toward both physisorption and chemisorption of the inhibitors on the metal surface.

4 Conclusion

- The polymers tested show good inhibitive effects on steel corrosion in 2 M H_3PO_4 and their inhibition efficiencies increase with concentration.

Table 5 The values of activation parameters (E_a, ΔH^{o}_{a}, ΔS^{o}_{a}) for steel in 2 M H_3PO_4in the absence and the presence of polymers 1 and 2

	Pre-exponential factor (mg cm^{-2} h^{-1})	Linear regression coefficient	E_a (kJ mol^{-1})	ΔH^{o}_{a} (kJ mol^{-1})	ΔS^{o}_{a} (J mol^{-1} K^{-1})
Blank	1.3901×10^{9}	0.997	51.32	48.65	–78.89
PVCVP	7.0653×10^{11}	0.997	70.56	67.88	–27.05
PVIVP	1.2631×10^{12}	0.998	72.85	70.18	–22.22

Table 6 Adsorption parameters of the linear regression between C (θ) and C of polymers 1 and 2

	Linear regression coefficient	K	ΔG^{o}_{ads} (kJ mol^{-1})
PVCVP	0.9994	987,761.6	–44.181
PVIVP	0.9998	1,339,175.7	–44.935

- The inhibitors act essentially in cathodic mode.
- PVCVP and PVIVP adsorb on steel from 2 M H_3PO_4 according to the Langmuir isotherm. The process is competitive between chemisorption and physical adsorption.
- The results obtained from different methods are in good agreement.

Acknowledgements The authors are grateful to Dr. E. E. Oguzie, Electrochemistry and Materials Science Research Laboratory, Federal University of Technology, Owerri, Nigeria, for reading through the manuscript.

References

1. Abed Y, Arrar Z, Aouniti A, Hammouti B, Kertit S, Mansri A (1999) J Chim Phys 96:1347
2. Annand RR, Hurd RM, Hackerman NJ (1965) Electrochem Soc 122:138
3. Abo El-Khair BM, Khalifa OR, Abedel-Hamid IA, Azzam AM (1983) Corros Prev Contr 34:15
4. Nikles DE, Warren GW (1998) Polym News 23:223
5. Jianguo Y, Lin W, Alego VO, Schweinsberg DP (1995) Corros Sci 37:975
6. Kim H, Jang J (1997) Polym Bull 38:249
7. Yongi DE, Nikles DE (2000) J Polym Sci 38:3278
8. Abed Y, Hammouti B, Touhami F, Aouniti A, Kertit S, Mansri A, Elkacemi K (2001) Bull Electrochem 17:105
9. Tuken T, Yazıcı B, Erbil M (2004) Prog Org Coat 51:152
10. Chetouani A, Medjahed K, Benabadji KE, Hammouti B, Kertit S, Mansri A (2003) Prog Org Coat 46:312
11. Chetouani A, Medjahed K, Sid-Lakhdar KE, Hammouti B, Benkaddour M, Mansri A (2004) Corros Sci 46:2421
12. Malik M, Wlodarczyk R, Kulesza P, Bala H, Miecznikowski K (2005) Corros Sci 47:771
13. Bentiss F, Traisnel M, Lagrenée M (2000) Corros Sci 42:127
14. Khaled KF (2003) Electrochim Acta 48:2493
15. Popova A, Christov M, Raicheva S, Sokolova E (2004) Corros Sci 46:1333
16. Wang L (2001) Corros Sci 43:391
17. Zhang D-Q, Gao L-X, Zhou G-D (2003) J Appl Electrochem 33:361
18. Dafali A, Hammouti B, Aouniti A, Mokhlisse R, Kertit S, Elkacemi K (2000) Ann Chim Sci Matér 25:437
19. Cruz J, Martínez R, Genesca J, García-Ochoa E (2004) J Electroanal Chem 566:111
20. Wang L, Pu J-X, Luo HC (2003) Corros Sci 45:677
21. Abd El-Maksoud SA, Fouda AS (2005) Mater Chem Phys 93:84
22. Tebbji K, Oudda H, Hammouti B, Benkaddour M, El Kodadi M, Ramdani A (2005) Appl Surf Sci 259:143
23. Xiao-Ci Y, Hong Z, Dao LM, Xuan RH, Lu-An Y (2000) Corros Sci 42:645
24. Bouklah M, Attayibat A, Hammouti B, Ramdani A, Radi S, Benkaddour M (2005) Appl Surf Sci 240:50
25. Lashkari M, Arshadi MR (2004) Chem Phys 299:131
26. Zhao TP, Mu GN (1999) Corros Sci 41:1937
27. Khamis E (1990) Corrosion 46:476
28. Li Z, Lu G, Huang J (2004) J Appl Polym Sci 94:2280
29. Manecke G, Stark M (1984) Die Makromol Chem 185:847
30. Martinez-Pina F, Gargalto L, Radic D (1998) Polym Int 47:340
31. Khaled KF, Babic-Samardzija K, Hackerman N (2006) Corros Sci 48:3014
32. Mansfeld F, Kending MW, Tsai S (1981) Corrosion 37:301, Ibid. 38 (1982) 570
33. McCafferty E, Hackerman N (1972) J Electrochem Soc 119:146
34. Bastidas JM, Polo JL, Cano E (2000) J Appl Electrochem 30:1173
35. Putilova IN, Balezin SA, Barannik VP (1960) Metallic corrosion inhibitors. Pergamon, Oxford
36. Popova A, Sokolova E, Raicheva S, Christov M (2003) Corros Sci 45:33
37. Saeed MT (2004) Anti-Corros Mater Meth 51:389
38. Mu GN, Li XM, Li F (2004) Mater Chem Phys 86:59
39. Gomma MK, Wahdan MH (1995) Mater Chem Phys 39:209
40. Khamis E, Hosney A, El-Khodary S (1996) Afinidad Rev Quim Teor Aplic 456:95
41. Tang L, Li X, Li L, Qu Q, Mu G, Liu G (2005) Mater Chem Phys 94:353
42. Donahue FM, Nobe K (1965) J Electrochem Soc 112:886
43. Khamis E, Bellucci F, Latanision RM, El-Ashry ESH (1991) Corrosion 47:677